Science of the Total Environment 658 (2019) 1475–1484

Contents lists available at ScienceDirect

Science of the Total Environment

journal homepage: www.elsevier.com/locate/scitotenv

Coupled hydrogeochemical evaluation of a vulnerable karst aquifer impacted by septic effluent in a protected natural area

Pingheng Yang [a,b,*], Ying Li [a], Chris Groves [b], Aihua Hong [c]

[a] Field Scientific Observation & Research Base of Karst Eco-Environments at Nanchuan in Chongqing, Ministry of Natural Resources of the People's Republic of China, School of Geographical Sciences, Southwest University, Chongqing 400715, China
[b] Crawford Hydrology Laboratory, Department of Geography and Geology, Western Kentucky University, Bowling Green, KY 42101, USA
[c] The Laboratory of Chongqing Groundwater Resource Utilization and Environmental Protection, Chongqing 401121, China

HIGHLIGHTS

- Concentrated inputs of septic effluent on karst aquifers have seldom been assessed.
- Artificial tracer tests, geochemistry, and dual nitrate isotopes were employed.
- The karst aquifer characterized by conduit system is highly vulnerable.
- Episodic release of septic effluent resulted in water quality deterioration.
- The study provides a basis for the development of groundwater protection schemes.

GRAPHICAL ABSTRACT

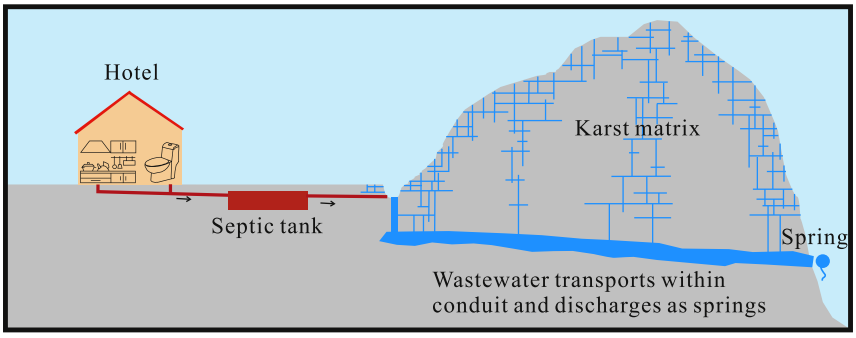

ARTICLE INFO

Article history:
Received 15 October 2018
Received in revised form 26 November 2018
Accepted 11 December 2018
Available online 12 December 2018

Editor: José Virgílio Cruz

Keywords:
Karst aquifer vulnerability
Tourism activities
Wastewater
Artificial tracer test
Geochemistry
Dual isotopes

ABSTRACT

Karst aquifers are highly vulnerable to pollution from human activities. Among sources of these contaminants, septic tank effluent can easily pollute karst aquifers, especially concentrated inputs such as those, for example, from tourist hotels. However, the impacts of septic effluent from relatively large, concentrated inputs on karst aquifers have seldom been assessed previously and therefore provide the focus of this study. Artificial tracer tests, geochemical analysis, and dual nitrate stable isotopes were employed to evaluate the impacts of a concentrated input of septic effluent from the Jinfoshan Holiday Hotel (JHH) on the vulnerable Shuifang Spring (SFS) karst aquifer in a remote mountainous area, the Jinfoshan Karst World Heritage Site within Chongqing Municipality of southwest China. The results of artificial tracer tests showed that the underground flow mainly occurred in a primary conduit with a pooled or bifurcated flow path that connects a sinkhole input to SFS. The high tracer recovery rates suggest that the karst aquifer was characterized by high intrinsic vulnerability to contamination. Chemographs at SFS responded rapidly to the episodic release of effluent from JHH. Decreased pH and dissolved oxygen and elevated turbidity, specific conductance and NH_4^+ concentrations of SFS resulted from the episodic release of septic tank effluent from the JHH during high-use periods. Although the nitrate concentrations were far below the guideline value of the Standard for Groundwater Quality of China, the isotopes of $\delta^{15}N_{NO3}$ and $\delta^{18}O_{NO3}$ suggest that nitrate flowing from SFS was primarily derived from manure and sewage, in addition to soil organic N. Thus, episodic release of septic effluent provides a challenge to the sustainability of karst groundwater management. The results of this study may be relevant to other remote and mountainous karst environments where tourism provide otherwise scarce economic resources and particularly to protected sites throughout the world.

* Corresponding author at: No. 2 Tiansheng Road, Beibei District, Chongqing 400715, China.
E-mail addresses: pinghengyang@126.com (P. Yang), chris.groves@wku.edu (C. Groves).

https://doi.org/10.1016/j.scitotenv.2018.12.172
0048-9697/

1. Introduction

Carbonate karst rocks outcrop over some 10–15% of the world's ice-free continental land area (Ford and Williams, 2007). Karst groundwater is an important freshwater resource that is used as a drinking water source by a significant proportion of the world's population (Ford and Williams, 2007). However, karst aquifers are highly vulnerable to pollution and have a very low natural self-purification capacity for most contaminants (e.g. Frank et al., 2018; Vesper et al., 2001). The development of sinkholes and fissures connecting the surface with the subsurface results in a discontinuous distribution and, in some cases, loss of the overlying surface soil layer, which can expose large areas of bedrock (Ford and Williams, 2007). Therefore, pollutants from the surface often undergo insufficient natural attenuation processes, like filtration and degradation through the soil layer, and they can rapidly enter the aquifer (e.g. Groves, 2018; Robinson and Hasenmueller, 2017). Simultaneously, well-developed karst conduits and associated high-velocity conduit flow along with a typically low storage capacity often provide insufficient time for purifying the pollutants in an aquifer (Butscher and Huggenberger, 2009; Marin et al., 2015). Consequently, these pollutants are often discharged along with groundwater at the underground river outlet or in the form of springs (e. g., Li et al., 2010; Mellander et al., 2012; Vesper and White, 2003), and can result in consistent, long term inputs to the groundwater within an aquifer (Lerch et al., 2018).

The use of in situ wastewater treatment systems, also known as septic tank systems, is a common wastewater treatment approach in rural and remote areas that lack the infrastructure needed for municipal wastewater treatment. Typical in situ wastewater treatment systems consist of two parts: a septic tank and a drain field (Toor et al., 2011). Due to their relatively simple design, septic tank systems can be a cost-effective and reliable means of removing contaminants from household wastewater before discharging it into the environment (Toor et al., 2011). Thus, septic tank systems have been extensively promoted throughout the world. Nevertheless, inadequate wastewater treatment by septic tank systems frequently leads to groundwater pollution incidents (USEPA, 2002). The loss of wastewater to the subsurface may occur deliberately through on-site septic tank systems or unintentionally, such as through leaks from disposal pipes (Withers et al., 2014). Therefore, the impact of septic tank systems on groundwater quality has caused widespread concern, particularly regarding the migration and fate of pollutants (Harden et al., 2008; Stanford et al., 2010).

Tourism has become an increasingly important type of recreation that stimulates local economic growth (Yang et al., 2009). However, infrastructure often cannot keep up with the rapidly growing number of tourists (Stanchev et al., 2015). This situation can result in negative impacts, such as air pollution (Saenz-de-Miera and Rosselló, 2014), solid waste pollution (Kaseva and Moirana, 2010), hydrocarbon pollution (Medina-Moreno et al., 2014), degradation of the color of scenic travertine (Simsek et al., 2000), and flowstone precipitation in tourist caves (Sebela and Turk, 2014), which present significant challenges to the sustainable development of tourism resources. Scenic karst areas often contain rich tourism resources. Increasing exploitation of karst resources is causing severe environmental degradation due to the fragility and vulnerability of karst areas (Sebela and Turk, 2014; Simsek et al., 2000). Wastewater discharge due to tourism activities in these areas can cause significant problems to these highly vulnerable karst groundwater and cave systems, but relevant documentation is rare (e.g. Yang et al., 2018).

Artificial tracer tests between sinkholes and karst springs have provided a scientific basis for quantitatively characterizing aquifer media properties, since this methodology for groundwater tracing in karst aquifers is well developed (Geyer et al., 2007). The results of tracer tests can lay the foundation for analyzing the vulnerability of karst aquifers (Goldscheider et al., 2003; Nguyet and Goldscheider, 2006). Hydrochemistry is a major indicator of water quality and is an important approach to study water circulation and the hydrogeological characteristics of aquifers (Gondwe et al., 2010; Yang et al., 2010). Nitrate pollution can originate from multiple sources via different pathways as point or diffuse sources: mineral nitrogen fertilizers and animal manure in agriculture, domestic or industrial nitrogen-bearing wastewater, atmospheric deposition, mineralization of soil organic nitrogen and biological nitrogen fixation (Kendall and Aravena, 2000; Nestler et al., 2011). Because isotopes of ^{15}N and ^{18}O have relatively stable characteristics, they can be used as fingerprints for tracing environmental nitrate pollution, regardless of the temporal and geographic scales. Dual isotopes of $\delta^{15}N_{NO3}$ and $\delta^{18}O_{NO3}$ in particular have been used to discriminate between organic (e.g. human or animal manure) and inorganic (e.g. chemical fertilizers) N contaminants in water (e.g. Grimmeisen et al., 2017; Hales et al., 2007; Musgrove et al., 2016; Weng et al., 2017).

Inscribed into the UNESCO World Heritage List in 2014, the Jinfoshan Karst (JFK) attracts 700,000 visitors per year, and is intensively visited by tourists during holiday and festival periods, resulting in generating a large amount of hotel wastewater at the Jinfoshan Holiday Hotel (JHH) that is treated by a septic system. This study uses the Shuifang Spring karst watershed, which is located in the core of the JFK, as a case study and the peak tourist season as the study period. We extend earlier work using stable hydrogen and oxygen isotopes (Yang et al., 2018) to apply geochemical analysis based on high-resolution data and dual nitrate stable isotopes to evaluate the impacts of a concentrated input of septic effluent from the JHH on the vulnerable karst aquifer. The objectives of this study were (1) to assess the hydraulic connection and intrinsic vulnerability of the karst aquifer based on artificial tracer tests, and (2) to analyze the impacts of episodic effluent release from the tourism hotel on karst groundwater on the basis of geochemical and stable nitrogen and oxygen isotope characteristics. Widespread global tourism activities and their production of wastewater, including impacts on the vulnerable karst flow systems of many World Heritage Sites and other protected areas, coupled with the prevalence of septic systems worldwide, suggest that this study may be relevant to other remotely mountainous and protected karst aquifers throughout the world.

2. Material and methods

2.1. Study area

The JFK lies in southern Chongqing, China (Fig. 1). The study area has a humid monsoon climate and is in the subtropical zone. Because of its relatively high elevation, the JFK spans a range of vertical climatic zones. The upper part of the mountain over 2000 m in elevation has a locally temperate humid climate, often with clouds and mist, little sunshine, abundant rainfall, and high humidity. The mean annual temperature and precipitation are 8.2 °C and 1434.5 mm, respectively.

The JFK is developed within Permian carbonate rocks. In the geological past, a basin in this region covered a large area with abundant rainfall and well-developed underground river systems. With topographic uplift due to neotectonic movements, river capture and headward erosion have destroyed the original drainage basin configuration. Currently, only the tableland surface remains at the upper part of the mountain, and the historical underground rivers have evolved into abandoned, dry caves, such as Xiannv Cave, Gufo Cave and Yangkou Cave (Fig. 1). Under modern climate conditions, a series of karst landforms, such as depressions and sinkholes (Fig. 1), has formed on the tableland surface. An underground river has also developed, which has an obvious entrance at Sinkhole #1 (elevation of ~2090 m) and an outlet at Shuifang Spring (SFS; elevation of 2053 m) at the edge of a large cliff (Fig. 1). Because the underground river is too small to be entered, a hypothesized route connected indicated by a linear collection of sinkholes was drawn as the extension of the underground river. The straight-line, lateral distance between Sinkhole #1 and SFS is ~526 m. SFS is

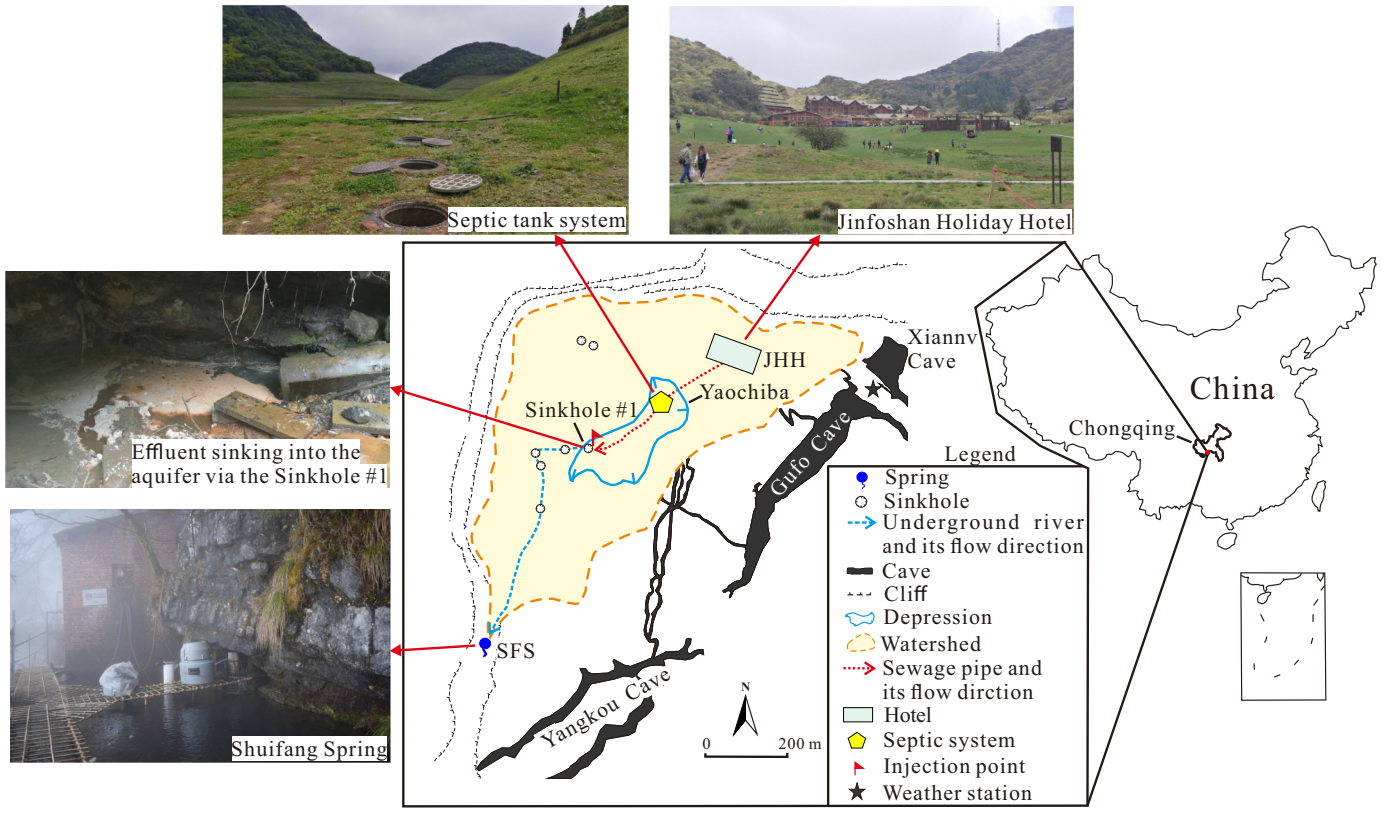

Fig. 1. Location of the study area and a schematic hydrogeological map. Hydrogeological information was modified from Wu et al. (2008).

recharged by the quick recharge through conduits and slow and low inflow from the fissured aquifer matrix (Wu et al., 2008). The discharge of SFS ranges from 0.5 to 38 L/s with an average of 6.5 L/s (Jiang et al., 2013). The shortest measured lag time of SFS peak flow in response to a rainstorm is only 2 h (Wu et al., 2008). The outflow of SFS pours down along the cliff and forms a stream for irrigation and sightseeing in its middle and downstream sections. In addition, a portion of water from SFS is pumped for artificial snow during the winter for tourist-based skiing. More hydrogeological information about the study area was reported by Jiang et al. (2013) and Wu et al. (2008).

In 2014, the JFK was designated as part of Phase II within the existing UNESCO "South China Karst World Heritage Site" (UNESCO, 2014). The JFK is a popular tourist destination in Southwest China and was ranked as a national 5A scenic spot in 2013, the highest ranking for the most important and best maintained sites in China. Every year, many tourists visit the JFK for sightseeing, skiing and enjoying the cooler climate of the higher elevations. The Jinfoshan Holiday Hotel (JHH) is located in the core area of the JFK and has a total of 96 rooms and 195 beds as well as a restaurant that accommodates 620 people. The water from Xiannv Cave (Fig. 1) supplies the domestic needs of the hotel. This source water has had relatively little human impact, as revealed by its nitrogen and oxygen isotopic compositions (see Section 3.3). The wastewater generated by the hotel is treated in a septic tank with a volume of ~120 m^3. The effluent, which acts as a point source, is episodically discharged into the karst aquifer through Sinkhole #1 (Fig. 1). In the absence of rain, it takes an estimated 26.8 h for water flushed down a toilet at JHH and processed through the septic tank to reach SFS (Yang et al., 2018).

2.2. Research methods

To fully constrain the vulnerability of the SFS basin karst aquifer being impacted by the septic effluent from the JHH, three hydrogeochemical methods — tracer tests, geochemistry, and nitrogen and oxygen isotopes — were employed, and their results were compared for verification.

2.2.1. Tracer tests

The aim of the artificial tracer tests was to investigate the hydraulic connection between Sinkhole #1 and SFS as well as features of the karst aquifer. Sodium fluorescein (uranine, $C_{20}H_{10}O_5Na_2$) and tinopal CBS-X ($C_{28}H_{20}S_2O_6Na_2$), both fluorescent dyes, were selected as tracers. They have been widely used in tracer tests in karst aquifers (e.g. Geyer et al., 2007; Licha et al., 2013; Magal et al., 2013). Tinopal CBS-X is an optical brightener dye that fluoresces at markedly shorter wavelengths and can easily be distinguished from sodium fluorescein (Goldscheider et al., 2008).

A GGUN-FL30 automatic field fluorometer (Albillia Sarl, Switzerland; Schnegg and Costa, 2002) was placed at SFS to determine the concentrations of the dyes as they emerged from the spring, which were plotted over time as tracer breakthrough curves (BTCs). The detection limits of sodium fluorescein, tinopal CBS-X and turbidity are 0.01 μg/L, 0.1 μg/L and 0.01 NTU, respectively, and they had a measurement interval of 5 min. A total of 100.6 g of sodium fluorescein and 161.9 g of tinopal CBS-X were mixed with water in a 50 L plastic bucket and simultaneously injected into Sinkhole #1 at 14:40 on 1/17/2017. The tracer test was finished at 12:45 on 2/14/2017. Table 1 summarizes the results of the tracer tests. The tracer recovery rate was calculated by multiplying the tracer concentration by the discharge (for the measurement method, see Section 2.2.2). Lateral distances in karst areas often require correction for sinuosity by a factor of approximately 1.5 based on the straight-line (Field, 2002). The estimated distance from Sinkhole #1 to SFS based on this correction factor was calculated as 789 m (Table 1).

2.2.2. Field sampling and monitoring

The physico-chemical parameters in the SFS watershed during high tourism periods of winter and summer (i.e., the 2015 Festival of Ice and

Table 1
Tracer test results.

Injection time	Tracer	*M* (g)	*D* (m)	*tf* (h)	*mv* (m/h)	*tm* (h)	*dv* (m/h)	*R* (%)
14:40 on 1/17/2017	Sodium fluorescein	100.6	789	24.5	32.2	42.8	24.5	97.3
14:40 on 1/17/2017	Tinopal CBS-X	161.9	789	26.1	30.2	47.6	16.6	70

M: mass of injected tracer; *D*: corrected distance between the injection point and the spring; *tf*: time of the first detection of the tracer; *mv*: maximum velocity; *tm*: time of detection of the maximum concentration; *dv*: dominant apparent flow velocity; *R*: tracer mass recovery.

Snow from late December 2014 to January 2015 as well as the 2016 summer season from July to early September 2016) were measured. The pH, specific conductance (spC), dissolved oxygen (DO), turbidity, and stage of SFS were automatically recorded using a Manta 2 multi-parameter water quality recorder (Eureka, USA) with a measurement interval of 10 min. The measurement accuracies of the pH, spC, DO, turbidity, Cl^-, and water stage were 0.01, 0.1 μS/cm, 0.1 mg/L, 0.1 NTU, 0.1 mg/L, and 0.01 mm, respectively. The discharge was converted from the water stage using a rating curve, which is expressed as the following empirical formula: $Q = 1.86\,Bh^{2/3}$ (Wang, 2011), where Q is the discharge (m^3/s), B is the weir width of SFS with a value of 0.3 m, and h is the water stage of SFS (m).

The data logger monitored physico-chemical parameters at SFS during two periods. The 2015 Festival of Ice and Snow interval produced 5223 data points, and 4013 data points were accumulated in the 2016 summer season. All of the electrodes/probes were calibrated before use in the field.

Manually collected samples and the automatically recorded data were concurrently analyzed for NH_4^+ and NO_3^-. From August 1 to September 18 in 2016, three water samples from the effluent were manually collected for analyses of NH_4^+ and NO_3^-, and 28 water samples from SFS were collected for analysis of NH_4^+, of which three were measured for NO_3^-.

To verify the results of tracer tests and geochemistry, a total of fourteen, two and fifteen samples for hotel water, effluent from Sinkhole #1, and water from SFS, respectively, were collected in 2017 and 2018 to determine the stable isotopic nitrogen and oxygen compositions. Water samples for isotopic analysis were filtered through a 0.22-μm mixed cellulose ester membrane in the field and stored in 40-mL brown polyethylene bottles. After pretreatment, the samples were stored at 4 °C and transported to the laboratory.

2.2.3. Analytical techniques

The $\delta^{15}N_{NO3}$ and $\delta^{18}O_{NO3}$ values were determined by TraceGas and Isotope Ratio Mass Spectrometry (IsoPrime, UK). The stable N and O isotope ratios are reported as the δ notation in parts per thousand (‰) relative to air N_2 and V-SMOW, respectively. For isotope value calibration, USGS KNO_3 reference materials with reported $\delta^{15}N_{NO3}$ and $\delta^{18}O_{NO3}$ values of 180‰ and 25.7‰ (USGS-32), −1.8‰ and −27.9‰ (USGS-34), and 2.7‰ and 57.5‰ (USGS-35), respectively, were used. The precision was <0.01‰. Replicate reproducibility was generally better than 0.4‰ for $\delta^{15}N_{NO3}$ and 0.22‰ for $\delta^{18}O_{NO3}$. The nitrogen and oxygen isotope data are presented in Supplementary document. The stable N and O isotope ratios were analyzed at the Agricultural Environmental Stable Isotope Laboratory of the Chinese Academy of Agricultural Sciences in Beijing, China.

The NH_4^+ and NO_3^- concentrations were determined in situ immediately after collection using a DR2800 spectrophotometer (Hach, USA), which had accuracies of 0.01 mg/L, and 0.01 mg/L, respectively. The HCO_3^- and Ca^{2+} concentrations were measured in situ by titration using a field alkalinity test kit (Merck, Germany) with accuracies of 0.1 mmol/L and 2 mg/L, respectively. Measurement of major ions was carried out at the Laboratory of Geochemistry and Isotopes at Southwest University in Chongqing, China. The measurements were made according to the methods described by Yang et al. (2010).

The amount of rainfall during the 2015 Festival of Ice and Snow was recorded by a HOBO weather station (Campbell, USA), whereas the rainfall and maximum air temperature during the 2016 summer season in the main urban area of Chongqing were downloaded from Accuweather (AccuWeather, 2017).

2.2.4. Visitor numbers

Visitor number data were obtained from the Administration Committee of the Jinfoshan Karst.

2.2.5. Data processing

The partial pressure of CO_2 (P_{CO2}) and the saturation index of calcite (SI_C) were calculated from the water temperature, pH, and concentrations of calcium, bicarbonate, potassium, sodium, magnesium, chlorine and sulfate using PHREEQC 3 (Parkhurst and Appelo, 2013). The relationships between the selected physico-chemical parameters were determined by Spearman's rank correlation coefficient in SPSS 19.0.

3. Results and discussion

3.1. Constraints from tracer tests

Tracing techniques can be used in all types of hydrological and hydrogeological environments to obtain information about groundwater movement and contaminant transport (Käss, 1998), but are especially useful in karst settings due to relatively rapid groundwater flow velocities. The BTCs obtained from the tracer tests are shown in Fig. 2. The tracer tests allowes estimation of relative groundwater velocities. The dominant apparent flow velocity (*dv*) was calculated based on the time of the maximum concentration (*tm*) on the BTCs, and the maximum flow velocity (*mv*) was calculated from the time that the tracer was first detected (*tf*). According to results of the two tracer tests, the *tf* values of sodium fluorescein and tinopal CBS-X in SFS were 24.5 and 26.1 h, respectively, and the *tm* values of sodium fluorescein and tinopal CBS-X were 42.8 and 47.6 h, respectively. Therefore, the *mv* values from Sinkhole #1 to SFS were 32.2 and 30.2 m/h, respectively, and the *dv* values were 24.5 and 16.6 m/h, respectively (Table 1). We propose that the fluorescein arrived at SFS before the tinopal CBS-X because tinopal CBS-X is thought to be a non-conservative tracer due to a

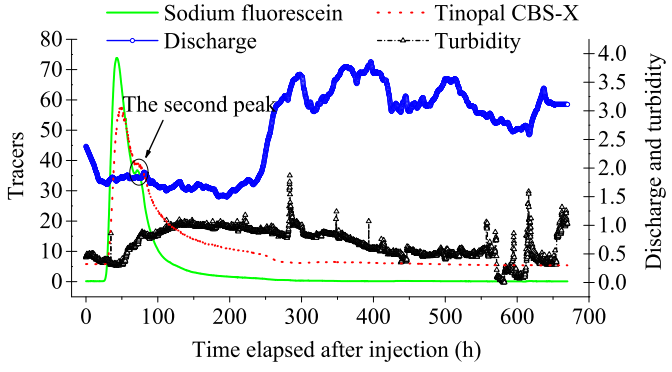

Fig. 2. Breakthrough curves of the dye tracer tests. The double-peak curves of the BTCs indicate a main conduit with a pool or an auxiliary conduit (a bifurcated flow path) between Sinkhole #1 and SFS. Tracers are in μg/L, discharge is in L/s, and turbidity is in NTU.

possibility of the precipitation of abundant cations Ca^{2+} and Mg^{2+} in groundwater (Geyer et al., 2007; Licha et al., 2013).

The tracer recovery rates of 97.3% and 70% for sodium fluorescein and tinopal CBS-X (Table 1), respectively, demonstrate that most of the mass of the injected tracers was recovered, which suggests that SFS was the main drainage outlet for the water flowing through Sinkhole #1. Due to the non-conservative characteristics of Tinopal CBS-X (Geyer et al., 2007; Licha et al., 2013), the recovery rate of tinopal CBS-X (70%) was much lower than that of sodium fluorescein (97.3%) at the same injection and monitoring site. In addition, tinopal CBS-X could have optical interference with DOC in the water (Goldscheider et al., 2008). Despite the recognized limitations of tinopal CBS-X as a hydrologic tracer agent, it was used as a tracer in this study so two tracers could be used to verify the hydraulic connections between Sinkhole #1 and SFS at the same time under the same hydrological conditions.

Double-peaked recovery curves of sodium fluorescein and tinopal CBS-X both were recorded at SFS (Fig. 2). Field and Leij (2012) noted that multiple peaks on a BTC can indicate the presence of pools or auxiliary conduits (bifurcated flow paths) in a karst aquifer, whereas a symmetrical BTC with a single peak indicates the presence of a single conduit. However, retention of a tracer and remobilization can also lead to multiple peaks, normally associated with a runoff event (Goldscheider et al., 2008). Obviously, the steady conditions (relatively steady discharge, stable and low level of turbidity) during the dual tracer peaks (Fig. 2) indicate that retention and remobilization in the aquifer was unlikely. The double-peak BTCs of the two tests thus likely indicate the existence of a main conduit with a pooled or a bifurcated flow path from Sinkhole #1 to SFS. Geomorphological observations based on the spatial arrangement of four sinkholes between Sinkhole #1 and SFS (Fig. 1) further confirmed the existence of a karst conduit with a cave stream that connects Sinkhole #1 and SFS.

High groundwater vulnerability is expected in zones where hydraulic connection and contaminant transport are possible (Goldscheider et al., 2003). This combination conduit system with a high tracer recovery suggests high intrinsic vulnerability of the karst aquifer between Sinkhole #1 and SFS. The hydrologic setting makes it possible to analyze the karst aquifer based on the assumption that the septic tank effluent recharges SFS via the conduit system.

3.2. Constraints from geochemistry

In karst groundwater, graphs showing variations or changes in chemical concentrations over time, called chemographs, often show rapid and strong responses to hydrologic events and contaminant release (Desmarais and Rojstaczer, 2002; Mahler and Massei, 2007; Vesper and White, 2003). Fig. 3 shows the chemographs of SFS during the periods of the 2015 Ice and Snow Festival and the 2016 summer season. The 2015 Ice and Snow Festival began on December 20, 2014. Between December 12, 2014 and January 6, 2015, 24.5 mm of rainfall was recorded (Fig. 3a). During the summer of 2016, as the maximum daily air temperature in the main urban area of Chongqing (nearly 2000 m lower in elevation that the top of Jinfoshan, and thus much warmer) gradually increased from 33 °C on August 1 to 42 °C on August 25, an accumulated number of 23477 visitors with a daily average of 939 people flocked to the JFK to avoid the heat wave (Fig. 3b). Only 10 mm of rain fell from August 2 to 25, 2016. The discharge decreased due to drought and hot weather before August 25 and was stable after August 25 due to slight rainfall. The maximum daily air temperature suddenly decreased from August 26. During the period August 26–31, there were only 1399 tourists with a daily average of 233 people visiting the JFK.

The hydrochemical parameters at SFS showed a high degree of variability during the study period (Fig. 3), which is typical of karst springs (Ford and Williams, 2007). Specifically, during the 2016 summer season, even though the high-resolution data of pH, DO, turbidity and spC lagged the peak air temperature about 1–2 days, because it took 26.8 h for JHH wastewater to arrive at SFS as revealed by tracer testing (Yang et al., 2018), the maxima of NH_4^+, NO_3^-, turbidity and spC and the minima of pH and DO in SFS and the effluent correlated with the peak air temperature on August 25 (Fig. 3b). The chemographs suggest that the groundwater quality of SFS episodically responded to the contaminant release resulting in deterioration.

Increased DO and increased clarity (lower turbidity) are typically associated with high water quality, whereas increased biological oxygen demand and turbidity are typically associated with low water quality (Tornevi et al., 2014; Lee and Lee, 2015). The water quality of SFS deteriorated during the study period along with a decline in DO and increased turbidity (Fig. 3), and negative correlation coefficients of −0.845 and −0.883 between them were observed for the 2015 Ice and Snow Festival and the 2016 summer season, respectively (Table 2). During the 2015 Festival of Ice and Snow, the turbidity of SFS sharply increased from ~0 NTU on 12/19/2014 to ~137 NTU on 12/26/2014 and remained at that level for approximately eight days until 1/3/2015 (Fig. 3a). During the 2016 summer season, the turbidity peaked on August 26 (Fig. 3b). In karst aquifers, turbidity is usually considered a parameter that indicates sediment transport from surface soils by overland flow during rainfall events, which results in strong positive correlations between turbidity and discharge/stage (Atteia and Kozel, 1997; Vesper and White, 2003). However, the turbidity trends were inconsistent with the variations in discharge (Fig. 3), with correlation coefficients of −0.665 and −0.553 for the 2015 Festival of Ice and Snow and the 2016 summer season, respectively (Table 2). In the two studied periods, the rainfall amount was small, resulting in a reduction or stabilization of the SFS discharge (Fig. 3). In addition, the wastewater produced by tourists contributed a mean value of ~18% to the flow discharge for SFS, which was calculated using a two-component mass balance equation of stable hydrogen and oxygen isotopic compositions (Yang et al., 2018). Therefore, the increased amount of effluent in the SFS basin probably did not exceed the reduced volume of recharge from rainfall, which resulted in a negative relationship between discharge and turbidity. The negative relationship between turbidity and discharge demonstrates that the increased turbidity of SFS was caused by the septic effluent from the JHH and slight rainfall recharge rather than by sediment transport in the conduit system as a result of rainfall.

Human activities can increase pollutant concentrations and decrease pH in groundwater (e.g. Heinz et al., 2009; Kelly et al., 2009). The spC of SFS increased with decreased pH and DO (Fig. 3) with correlation coefficients of −0.897 and −0.902 between the spC and pH and −0.819 and −0.924 between the spC and DO for the 2015 Ice and Snow Festival and the 2016 summer season, respectively (Table 2). Effluent typically contains large amounts of organic matter and microorganisms (Heinz et al., 2009; Kelly et al., 2009). Microorganisms can decompose organic matter with oxygen consumption and produce large amounts of CO_2 dissolved in water, as is shown by the elevated P_{CO2} in the groundwater of SFS during the period 12/23/2014–1/4/2015 (Fig. 4). According to studies by Kogovšek and Petrič (2013) and Kogovšek (2011) in the karst region of southern Slovenia, karst porous media were dissolved by the inorganic acid in landfill filtrate, resulting in aquifer flow paths being enlarged and an increase in the permeability of the vadose. As a result, the pH of SFS decreased, and the groundwater became more undersaturated, with a decrease in SI_C (Fig. 4) that may suggest that the effluent transported in the aquifer potentially promoted the dissolution of the carbonate bedrock of the conduits. Consequently, the concentrations of Ca^{2+} and HCO_3^- and the spC in the groundwater increased to some extent (Fig. 3a). Organic pollutants in the effluent probably entered a state of anaerobic decomposition with a decrease in DO (Fig. 3), which may generate H_2S, CH_4 and other reducing gases. The effluent, which is rich in organic pollutants and gases, resulted in the black water, with a dramatic increase in turbidity (Fig. 3). This interpretation is supported by the elevated turbidity, coupled with decreased DO (Fig. 3) and their negative correlation (Table 2).

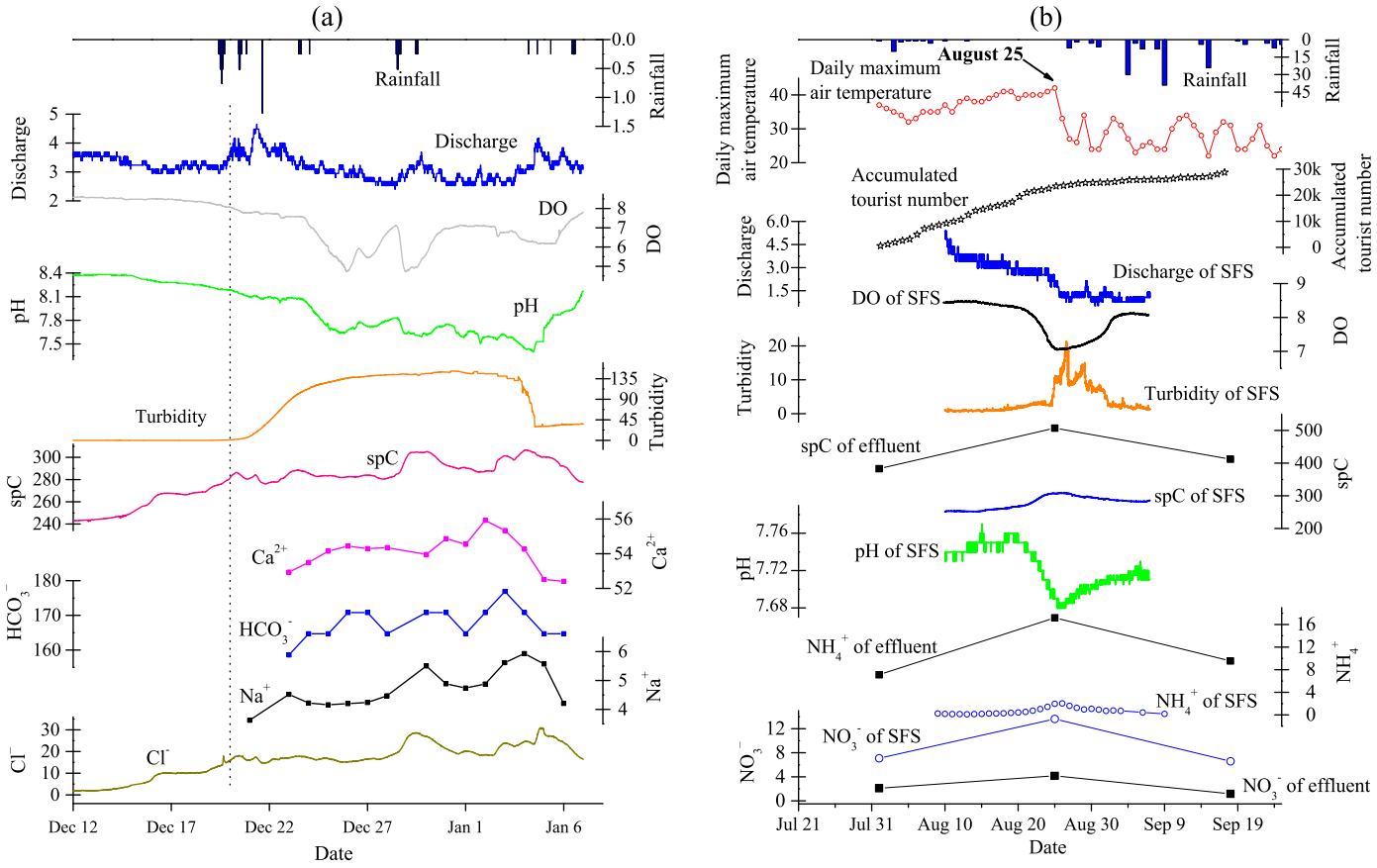

Fig. 3. (a) Chemographs and rainfall for SFS during the 2015 Festival of Ice and Snow and (b) rainfall, air temperature, discharge, and chemographs for SFS and effluent during the 2016 summer season. The first day of the 2015 Festival of Ice and Snow is indicated by the black dashed line. The variations in the physico-chemical parameters suggest that the episodic release of effluent affected and caused deterioration of the water quality of SFS. Rainfall is in mm; temperature is in °C; turbidity is in NTU; discharge is in L/s; spC is in μS/cm; and the major elements are in mg/L.

The peak concentrations of NH_4^+ and NO_3^- in SFS and the effluent correlated with the maximum air temperature in the 2016 summer season (Fig. 3b), which also suggests that the effluent significantly deteriorated the groundwater quality at SFS. Tourists flocked to the JFK to avoid the heat wave and produced wastewater, which resulted in elevated NO_3^- and NH_4^+ concentrations at both SFS and Sinkhole #1 before August 25. Because the air temperature dropped after August 25, the number of tourists was reduced, and the concentrations of NO_3^- and NH_4^+ decreased correspondingly (Fig. 3b). It should be noted that the mean concentrations of NH_4^+ and NO_3^- in the effluent were 11.3 mg/L and 2.5 mg/L, respectively (Fig. 3b), and the NH_4^+ content was nearly six times higher than that of NO_3^-. After ammonification or mineralization in a septic tank, the nitrogen in the septic tank effluent is often largely in the form of NH_4^+ (Zhu et al., 2016), which renders the effluent rich in NH_4^+ and poor in NO_3^-. The reason for the higher NH_4^+ probably is

Table 2
Correlation coefficients between the selected physico-chemical parameters of SFS during the 2015 Festival of Ice and Snow and the 2016 summer season. The number in brackets is the correlation coefficient for the 2016 summer season. A total of 5223 data points from the 2015 Festival of Ice and Snow and 4013 data points from the 2016 summer season were used for the calculations.

	pH	spC	Turbidity	Cl^-	DO	Discharge
pH	1	−0.897[a] (−0.902[a])	−0.894[a] (−0.767[a])	−0.889[a]	0.903[a] (0.901[a])	0.652[a] (0.763[a])
spC		1	0.767[a] (0.734[a])	0.988[a]	−0.819[a] (−0.924[a])	−0.730[a] (−0.759[a])
Turbidity			1	0.739[a]	−0.845[a] (−0.883[a])	−0.665[a] (−0.533[a])
Cl^-				1	−0.821	−0.680[a]
DO					1	0.597[a] (0.639[a])
Discharge						1

[a] Correlation is significant at α = 0.01 level (2-tailed).

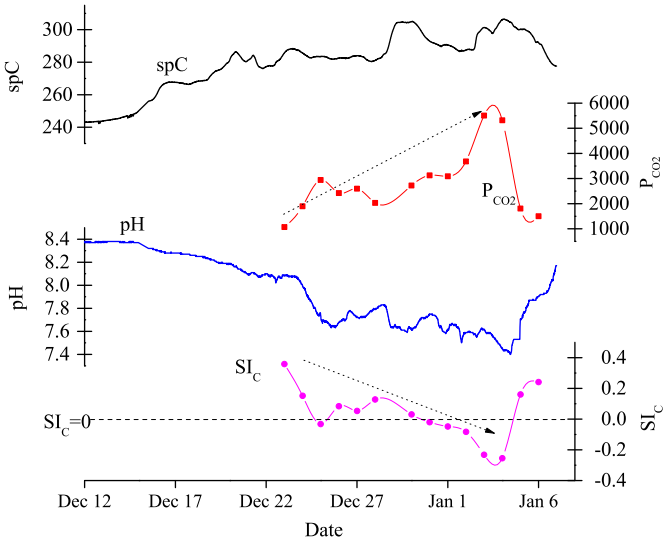

Fig. 4. Variations in selected physico-chemical parameters of SFS during the 2015 Ice and Snow Festival. The increase in P_{CO2} and decrease in SI_C suggest that SFS was recharged by the effluent, which contained high concentrations of CO_2 produced by microorganisms. spC is in μg/L; P_{CO2} is in ppmv.

that dissimilatory nitrate reduction to ammonium (DNRA) which may provide a mechanism for the temporary attenuation of nitrate in the groundwater (Rivett et al., 2008). While typical levels of NH_4^+ do not pose a direct risk to human health (Umezawa et al., 2008), elevated NH_4^+ levels suggest the presence of more serious contaminants (Zhang and Zhang, 2007), such as pathogens, pharmaceuticals, personal care products, cleaning products or pesticides.

The mean concentrations of NH_4^+ and NO_3^- at SFS were 0.70 mg/L and 9.1 mg/L, respectively (Fig. 3b). The NO_3^- concentrations in SFS were within the threshold value of 89 mg-NO_3^-/L (20 mg-nitrogen/L) according to the *Standard for Groundwater Quality* (GAQS and IQPRC, 2017). The mean NH_4^+ content at SFS was approximately 16 times lower than that of the effluent, whereas the NO_3^- concentration was almost four times higher than that of the effluent (Fig. 3b). This result is attributed to nitrification occurring in the karst conduit, where NH_4^+ from the effluent was quickly and completely oxidized back to NO_3^- by nitrification (Rivett et al., 2008) and mixing of relatively oxygen-rich groundwater (Grimmeisen et al., 2017). Therefore, due to the high vulnerability of the karst aquifer, the chemical components at SFS were at least partly unprotected against pollution from the effluents.

3.3. Constraints from dual isotopes of ^{15}N and ^{18}O in water

Denitrification is considered to be the most significant reaction impacting nitrate attenuation in the groundwater. Denitrification causes the $\delta^{15}N_{NO3}$ of the residual nitrate to increase exponentially as nitrate concentrations decrease (Kendall and Aravena, 2000). For example, denitrification of fertilizer NO_3^- with an original $\delta^{15}N_{NO3}$ value of +0‰ can yield residual $\delta^{15}N_{NO3}$ values (e.g. +15 to +30‰) that are within the range of the compositions expected for NO_3^- derived from a manure or septic tank source (Michener and Lajtha, 2007), making it difficult to identify the nitrate sources. Before tracing the sources of NO_3^- on the basis of coupled nitrate N and O isotope fingerprinting, it is good practice to determine whether denitrification has occurred in the water samples.

Typical values of $\delta^{15}N_{NO3}$ and $\delta^{18}O_{NO3}$ of nitrate derived or produced by nitrification from various N sources are plotted in Fig. 5, which can help us distinguish the NO_3^- sources in the study area. It has been established that the denitrification of NO_3^- results in a linear ratio of $\delta^{15}N/\delta^{18}O$ typically lying within a range of 1.3–2.1 (Aravena and Robertson, 1998; Fukada et al., 2003; Panno et al., 2006); i.e., the slopes of $^{18}O_{NO3}$ relative to $\delta^{15}N_{NO3}$ range from 0.48–0.76. The slopes of $^{18}O_{NO3}$ relative to $\delta^{15}N_{NO3}$ for JHH water and SFS were −0.94, 0.03, respectively, out of the range of 0.48–0.76, suggesting insignificant or negligible denitrification in the water samples from SFS and hotel water. This result at SFS is consistent with a previous study that suggests the nitrogen from belowground leaking sewers was less susceptible to denitrification (Kaushal et al., 2011). A ~2:1 linear increase in $\delta^{15}N_{NO3}$ and $\delta^{18}O_{NO3}$ at samples from Sinkhole #1 suggests that denitrification was a dominant process in the effluent, although there are only two data points (Fig. 5). This result is consistent with the low nitrate concentrations in the effluent at Sinkhole #1.

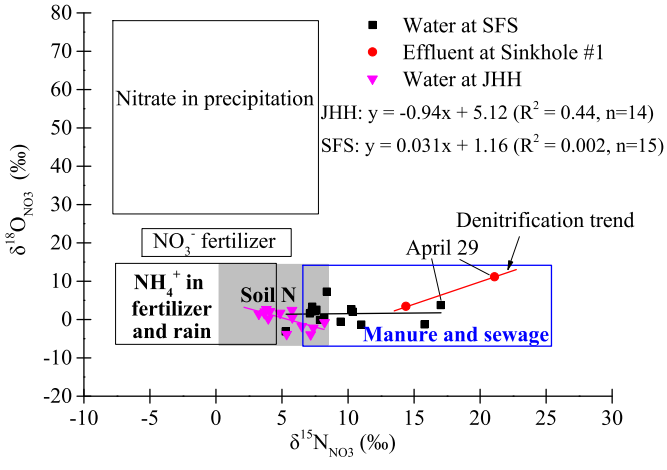

Fig. 5. Schematic for source identification based on $\delta^{15}N_{NO3}$ and $\delta^{18}O_{NO3}$ values. The bordered boxes delineate the typical ranges of $\delta^{15}N_{NO3}$ and $\delta^{18}O_{NO3}$ values for nitrate sources (Nestler et al., 2011; Kendall and Aravena, 2000). The nitrate in the hotel water was derived from the soil organic nitrogen. Manure and sewage contributed to the effluent nitrate. A mixture of manure, sewage and soil organic N was responsible for the nitrate at SFS.

The $\delta^{15}N_{NO3}$ and $\delta^{18}O_{NO3}$ values for JHH water ranged from 3.2‰ to 8.2‰ and from −3.9‰ to 2.7‰, respectively, which suggests that the NO_3^- was primarily derived from soil organic N or a mixture of soil organic N, NH_4^+ in fertilizer and rain, and manure and sewage (Fig. 5). However, agricultural activities are strictly forbidden in the study area. Furthermore, the altitude of the water source for JHH, Xiannv Cave, is covered by forest and is higher than that of JHH and its septic system. Thus, soil organic N is likely the main origin of nitrate in the hotel water, with a mean NO_3^- concentration of 4.9 mg/L, indicating that the water has not been impacted by human activities and has maintained the natural background condition.

The $\delta^{15}N_{NO3}$ and $\delta^{18}O_{NO3}$ values of the two effluent samples were 14.4‰ to 21.1‰ and 3.5‰ to 11.2‰, respectively, suggesting that manure and sewage contributed nitrate to the effluent (Fig. 5). The SFS samples contained $\delta^{15}N_{NO3}$ and $\delta^{18}O_{NO3}$ values that ranged from 5.3‰ to 17‰, and −3.1‰ to 7.3‰, respectively, suggesting the NO_3^- was derived from manure and sewage and a mixture of manure, sewage and soil organic N (Fig. 5). SFS is recharged by the effluent through conduit(s) from Sinkhole #1 and the fissured aquifer matrix. The effluent is characterized by quick recharge and high $\delta^{15}N_{NO3}$ values, while the fissured aquifer matrix is supplied by diffuse flow from the overlying thick soil layer (maximum of 18 m; Wu et al., 2008) and the epikarst zone. The soil water should have $\delta^{15}N_{NO3}$ and $\delta^{18}O_{NO3}$ values identical to those of the adjacent Xiannv Cave water, which supplies the hotel with water. The SFS water therefore likely represents a mixture of septic nitrate and non-septic background nitrate originating from the overlying soil. It should be noted that the occurrence of the high $\delta^{15}N_{NO3}$ value of 21.1‰ in the effluent on April 29, 2017, was likely because the azalea flowers were in full blossom (from the end of April to the middle of May), so visitors flocked to the JFK for sightseeing and produced a great amount of sewage. Additionally, SFS had a $\delta^{15}N_{NO3}$ value of 17.0‰ on April 29, 2017, corresponding to the sewage release from the septic tank system. The source of NO_3^- at SFS was calculated using a Bayesian isotopic mixing model, named the SIAR model (Parnell et al., 2010). The result indicates that the contribution rate of atmospheric precipitation, soil organic N, and manure sewage were roughly 29%, 36%, and 35%, respectively.

These findings on the basis of the stable nitrogen and oxygen isotopic compositions also indicate that SFS is highly vulnerable to the episodic release of sewage from the JHH.

3.4. Applications for groundwater protection

Our natural heritage consists of the legacy from the past, how we protect the world today, and what we pass on to future generations. The UNESCO World Heritage Convention identifies sites that have outstanding universal value, and which provide irreplaceable sources of life and inspiration (UNESCO, 2018a). A total of 54 properties of World Heritage List have been included on the list of World Heritage Sites in danger by the World Heritage Committee (UNESCO, 2018b). The World Heritage Site at the JFK has a unique karst and superlative tableland landscape and distinctive cave evolution processes. However, the tracer tests clearly demonstrated that the septic effluent produced by the JHH that enters Sinkhole #1 rapidly arrives at SFS, and the karst aquifer has high intrinsic vulnerability from these contaminants. As a result, the water quality in the groundwater system is affected by the

episodic septic effluent which is driven by the tourism activities. Although most of the ion concentrations are within the acceptable limits for drinking water, the issue of episodic release of septic tank effluent and its environmental impact on the karst aquifer probably has the potential to affect the integrity of the ecosystem of the JFK.

This finding has important practical significance for the future protection of groundwater systems and karst environments more broadly. Relevant administrative departments should be sensitive to and monitor the negative impacts of tourism activities on vulnerable karst groundwater systems and develop land use strategies that minimize pollution and ecological deterioration due to tourism development. Ecotourism is a growing trend in many countries that takes advantage of places where the natural environment is impressive enough to draw visitors. Best practices of ecotourism attempt to reduce negative anthropogenic impacts on these systems by limiting tourist numbers and reducing the building of infrastructure at these sites (Van Beynen et al., 2012). Vulnerability mapping appears to be an effective tool to assess karst aquifer vulnerability and has been proposed as a basis for protection zoning and land-use planning. These methods specifically developed for the assessment of vulnerability in karst areas include COP (Vías et al., 2006), PI (Goldscheider et al., 2000) and EPIK (Doerfliger et al., 1999). Thus, it is necessary to carry out vulnerability mapping in the JFK to protect the valuable karst groundwater resources.

Karst aquifers are especially vulnerable to microbial contamination (Buckerfield et al., 2019; Goeppert and Goldscheider, 2011; Nguyet and Goldscheider, 2006). Unfortunately, microbiological analyses typically require sterile water sampling, sample cooling, and rapid transport of the samples to a microbiological laboratory (Hurst et al., 2002). In remote areas such as the JFK, these requirements are very difficult to meet, and this study did not assess microbial contamination in the karst basin. However, Lettingue (2007) measured coliform bacteria at SFS in 2007 and found that an increase in bacteriological contamination with 158 thermotolerant coliforms per 100 mL induced by a high runoff event. It was suspected that the coliforms were derived from the wastewater of the tourist village without soil filtration. This suggests that the microbial contamination caused by tourism activities was quite serious at that time. Despite significant improvements in the sanitary quality of drinking water with technological and economic development, disease outbreaks continue to result from pathogen-contaminated groundwater (Borchardt et al., 2011; Yoder et al., 2010). For instance, in early June 2007, 229 patrons and employees of a new restaurant in northeastern Wisconsin, USA, were affected by acute gastroenteritis, and 6 people were hospitalized. Epidemiological, microbiological, and hydrogeological investigations proved that the restaurant's well water was polluted by a new septic system in a fractured dolomite aquifer and caused the illness (Borchardt et al., 2011). The minimal requirement, therefore, is for wastewater to be completely disinfected with chlorine or some other disinfectant before it is released back into the karst ecosystem. This study therefore highlights that the public perception that "mountainous karst springs are pristine and consequently safe to drink from" is not necessarily correct, as was also reported by Goeppert and Goldscheider (2011) and Nguyet and Goldscheider (2006), particularly during periods of episodic effluent release.

4. Conclusions

The unique characteristics of karst environments make them highly vulnerable to human disturbance. In this study, a combination of artificial tracer tests, geochemical analyses and stable nitrogen and oxygen isotopic compositions were used to constrain the vulnerability of the karst groundwater system of the SFS aquifer in the JFK, Southwest China. Due to its established conduit-dominated structure and as confirmed by high tracer recovery rates, the SFS karst groundwater system is particularly prone to contamination and highly vulnerable to the impacts of septic tank effluent from the JHH. The episodic release of contaminants from septic systems poses a threat to the water quality of SFS and results in enrichment of the $^{15}N_{NO3}$ and $^{18}O_{NO3}$ isotopes in the karst groundwater, and presents a challenge to the protection of the karst aquifer characterized by highly intrinsic vulnerability. Therefore, the managers need to develop reasonable policies and develop land use protection measures, such as ecotourism, and carry out vulnerability mapping for the whole protected natrual area. The combination of tracer tests, hydrochemical methods, and stable hydrogen and oxygen isotopic techniques make it possible to better understand the karst aquifer system and to characterize the dynamics and interaction of hydrologic, hydrochemical and isotopic parameters. This study also provides a basis for the development of future groundwater protection schemes.

Supplementary data to this article can be found online at https://doi.org/10.1016/j.scitotenv.2018.12.172.

Conflict of interest

The authors have no conflicts of interest to declare.

Acknowledgments

The authors express gratitude to their graduate students, including Feng Chen, Zhaojun Zhan, Juan Ren, Ting Sheng, Guowen Xie, Zhengliang Yu, Xiaoxing Ming, and Dan Luo, for their help with field work. The authors also thank Professor Nico Goldscheider (Karlsruhe Institute of Technology), and the anonymous reviewers for their constructive and valuable comments. This work was supported by the National Natural Science Foundation of China (41103068), the Fundamental Research Funds for the Central Universities (XDJK2018AB002, SWU116087, XDJK2014C114 and XDJK2017B13), and the China Scholarship Council.

References

AccuWeather, 2017. http://www.accuweather.com (accessed July 1, 2017).
Aravena, R., Robertson, W.D., 1998. Use of multiple isotope tracers to evaluate denitrification in ground water: study of nitrate from a large-flux septic system plume. Ground Water 36, 975–982. https://doi.org/10.1111/j.1745-6584.1998.tb02104.x.
Atteia, O., Kozel, R., 1997. Particle size distributions in waters from a karstic aquifer: from particles to colloids. J. Hydrol. 201, 102–119. https://doi.org/10.1016/S0022-1694(97)00033-4.
Borchardt, M.A., Bradbury, K.R., Alexander Jr., E.C., Kolberg, R.J., Alexander, S.C., Archer, J.R., Braatz, L.A., Forest, B.M., Green, J.A., Spencer, S.K., 2011. Norovirus outbreak caused by a new septic system in a dolomite aquifer. Ground Water 49, 85–97. https://doi.org/10.1111/j.1745-6584.2010.00686.x.
Buckerfield, S.J., Waldron, S., Quilliam, R.S., Naylor, L.A., Li, S., Oliver, D.M., 2019. How can we improve understanding of faecal indicator dynamics in karst systems under changing climatic, population, and land use stressors? - research opportunities in SW China. Sci. Total Environ. 646, 438–447. https://doi.org/10.1111/j.scitotenv.2018.07.292.
Butscher, C., Huggenberger, P., 2009. Enhanced vulnerability assessment in karst areas by combining mapping with modeling approaches. Sci. Total Environ. 407, 1153–1163. https://doi.org/10.1016/j.scitotenv.2008.09.033.
Desmarais, K., Rojstaczer, S., 2002. Inferring source waters from measurements of carbonate spring response to storms. J. Hydrol. 260, 118–134. https://doi.org/10.1016/S0022-1694(01)00607-2.
Doerfliger, N., Jeannin, P.Y., Zwahlen, F., 1999. Water vulnerability assessment in karst environments: a new method of defining protection areas using a multi-attribute approach and GIS tools (EPIK method). Environ. Geol. 39, 165–176. https://doi.org/10.1007/s002540050446.
Field, M.S., 2002. The QTRACER2 Program for Tracer-Breakthrough Curve Analysis for Tracer Tests in Karstic Aquifer and Other Hydrologic Systems. National Center for Environmental Assessment, Washington, D.C.
Field, M.S., Leij, F.J., 2012. Solute transport in solution conduits exhibiting multi-peaked breakthrough curves. J. Hydrol. 440–441, 26–35. https://doi.org/10.1016/j.jhydrol.2012.03.018.
Ford, D., Williams, P., 2007. Karst Hydrogeology and Geomorphology. Wiley, Chichester, U.K.
Frank, S., Goeppert, N., Goldscheider, N., 2018. Fluorescence-based multi-parameter approach to characterize dynamics of organic carbon, faecal bacteria and particles at alpine karst springs. Sci. Total Environ. 615, 1446–1459. https://doi.org/10.1016/j.scitotenv.2017.09.095.
Fukada, T., Hiscock, K.M., Dennis, P.F., Grischek, T., 2003. A dual isotope approach to identify denitrification in groundwater at a river-bank infiltration site. Water Res. 37, 3070–3078. https://doi.org/10.1016/S0043-1354(03)00176-3.
General Administration of Quality Supervision, Inspection and Quarantine of the People's Republic of China (GAQS and IQPRC), 2017. Standard for Groundwater Quality (GB/T 14848-2017) (in Chinese without English abstract).

Geyer, T., Birk, S., Licha, T., Liedl, R., Sauter, M., 2007. Multitracer test approach to characterize reactive transport in karst aquifers. Ground Water 45, 36–45. https://doi.org/10.1111/j.1745-6584.2006.00261.x.
Goeppert, N., Goldscheider, N., 2011. Transport and variability of fecal bacteria in carbonate conglomerate aquifers. Ground Water 49, 77–84. https://doi.org/10.1111/j.1745-6584.2010.00741.x.
Goldscheider, N., Klute, M., Sturm, S., Hötzl, H., 2000. The PI method – a GIS-based approach to mapping groundwater vulnerability with special consideration of karst aquifers. Z. Angew. Geol. 46, 157–166.
Goldscheider, N., Hötzl, H., Käss, W., Ufrecht, W., 2003. Combined tracer tests in the karst aquifer of the artesian mineral springs of Stuttgart, Germany. Environ. Geol. 43, 922–929. https://doi.org/10.1007/s00254-002-0714-9.
Goldscheider, N., Meiman, J., Pronk, M., Smar, C., 2008. Tracer tests in karst hydrogeology and speleology. Int. J. Speleol. 37, 27–40. https://doi.org/10.5038/1827-806X.37.1.3.
Gondwe, B.R.N., Lerer, S., Stisen, S., Marín, L., Rebolledo-Vieyra, M., Merediz-Alonso, G., Bauer-Gottwein, P., 2010. Hydrogeology of the south-eastern Yucatan Peninsula: new insights from water level measurements, geochemistry, geophysics and remote sensing. J. Hydrol. 389, 1–17. https://doi.org/10.1016/j.jhydrol.2010.04.044.
Grimmeisen, F., Lehmann, M.F., Liesch, T., Goeppert, N., Klinger, J., Zopfi, J., Goldscheider, N., 2017. Isotopic constraints on water source mixing, network leakage and contamination in an urban groundwater system. Sci. Total Environ. 583, 202–213. https://doi.org/10.1016/j.scitotenv.2017.01.054.
Groves, C., 2018. Editor's message: US Environmental Protection Agency's coal combustion residuals rule strengthens regulatory recognition of karst groundwater flow. Hydrogeol. J. 26, 361–365. https://doi.org/10.1007/s10040-017-1673-2.
Hales, H.C., Ross, D.S., Lini, A., 2007. Isotopic signature of nitrate in two contrasting watersheds of Brush Brook, Vermont, USA. Biogeochemistry 84, 51–66. https://doi.org/10.1007/s10533-007-9074-6.
Harden, H.S., Roeder, E., Hooks, M., Chanton, J.P., 2008. Evaluation of onsite sewage treatment and disposal systems in shallow karst terrain. Water Res. 42, 2585–2597. https://doi.org/10.1016/j.watres.2008.01.008.
Heinz, B., Birk, S., Liedl, R., Geyer, T., Straub, K.L., Andresen, J., Bester, K., Kappler, A., 2009. Water quality deterioration at a karst spring (Gallusquelle, Germany) due to combined sewer overflow: evidence of bacterial and micro-pollutant contamination. Environ. Geol. 57, 797–808. https://doi.org/10.1007/s00254-008-1359-0.
Hurst, C.J., Crawford, R.L., Garland, J.L., Lipson, D.A., 2002. Manual of Environmental Microbiology. Second edition. American Society for Microbiology Press, Washington, D.C.
Jiang, Y., Hu, Y., Schirmer, M., 2013. Biogeochemical controls on daily cycling of hydrochemistry and $\delta^{13}C$ of dissolved inorganic carbon in a karst spring-fed pool. J. Hydrol. 478, 157–168. https://doi.org/10.1016/j.jhydrol.2012.12.001.
Kaseva, M.E., Moirana, J.L., 2010. Problems of solid waste management on Mount Kilimanjaro: a challenge to tourism. Waste Manag. Res. 28, 695–704. https://doi.org/10.1177/0734242X09337655.
Käss, W., 1998. Tracing Technique in Geohydrology. Taylor & Francis, Rotterdam, Netherlands.
Kaushal, S.S., Groffman, P.M., Band, L.E., Elliott, E.M., Shields, C.A., Kendall, C., 2011. Tracking nonpoint source nitrogen pollution in human-impacted watersheds. Environ. Sci. Technol. 45, 8225–8232. https://doi.org/10.1021/es200779e.
Kelly, W.R., Panno, S.V., Hackley, K.C., Martinsek, A.T., Krapac, I.G., Weibel, C.P., Storment, E.C., 2009. Bacteria contamination of groundwater in a mixed land-use karst region. Water Qual Expo Health 1, 69–78. https://doi.org/10.1007/s12403-009-0006-7.
Kendall, C., Aravena, R., 2000. Nitrate isotopes in groundwater systems. In: Cook, P.G., Herczeg, A.L. (Eds.), Environmental Tracers in Subsurface Hydrology. Springer, Boston, MA https://doi.org/10.1007/978-1-4615-4557-6_9.
Kogovšek, J., 2011. Impact of chlorides, nitrates, sulfates and phosphates on increased limestone dissolution in the karst vadose zone (Postojna Cave, Slovenia). Acta Carsologica 40, 319–327. https://doi.org/10.3986/ac.v40i2.16.
Kogovšek, J., Petrič, M., 2013. Increase of vulnerability of karst aquifers due to leakage from landfills. Environ. Earth Sci. 70, 901–912. https://doi.org/10.1007/s12665-012-2180-3.
Lee, L.H., Lee, Y.D., 2015. The impact of water quality on the visual and olfactory satisfaction of tourists. Ocean Coast. Manag. 105, 92–99. https://doi.org/10.1016/j.ocecoaman.2014.12.020.
Lerch, R.N., Groves, C.G., Polk, J.S., Miller, B.V., Shelley, J., 2018. Atrazine transport through a soil-epikarst system. J. Environ. Qual. 47, 1205–1213. https://doi.org/10.2134/jeq2017.12.0492.
Lettingue, M., 2007. Vulnerability and Risk Mapping, Tracer Tests and Microbiological Monitoring to Assess the Human Impact on an UNESCO World Heritage Candidate Site, the Jinfo Karst Plateau, China. (Master Thesis). Université de Neuchâtel.
Li, X., Liu, C., Harue, M., Li, S., Liu, X., 2010. The use of environmental isotopic (C, Sr, S) and hydrochemical tracers to characterize anthropogenic effects on karst groundwater quality: a case study of the Shuicheng Basin, SW China. Appl. Geochem. 25, 1924–1936. https://doi.org/10.1016/j.apgeochem.2010.10.008.
Licha, T., Niedbala, A., Bozau, E., Geyer, T., 2013. An assessment of selected properties of the fluorescent tracer, Tinopal CBS-X related to conservative behavior, and suggested improvements. J. Hydrol. 484, 38–44. https://doi.org/10.1016/j.jhydrol.2013.01.006.
Magal, E., Arbel, Y., Caspi, S., Glazman, H., Greenbaum, N., Yechieli, Y., 2013. Determination of pollution and recovery time of karst springs, an example from a carbonate aquifer in Israel. J. Contam. Hydrol. 145, 26–36. https://doi.org/10.1016/j.jconhyd.2012.10.010.
Mahler, B., Massei, N., 2007. Anthropogenic contaminants as tracers in an urbanizing karst aquifer. J. Contam. Hydrol. 91, 81–106. https://doi.org/10.1016/j.jconhyd.2006.08.010.
Marin, A.I., Andreo, B., Mudarra, M., 2015. Vulnerability mapping and protection zoning of karst springs. Validation by multitracer tests. Sci. Total Environ. 532, 435–446. https://doi.org/10.1016/j.scitotenv.2015.05.029.
Medina-Moreno, S.A., Jimenez-Gonzalez, A., Gutierrez-Rojas, M., Lizardi-Jimenez, M.A., 2014. Hydrocarbon pollution studies of underwater sinkholes along Quintana Roo as a function of tourism development in the Mexican Caribbean. Rev. Mex. Ing. Quím. 13, 509–516.
Mellander, P.E., Jordan, P., Wall, D.P., Melland, A.R., Meehan, R., Kelly, C., Shortle, G., 2012. Delivery and impact bypass in a karst aquifer with high phosphorus source and pathway potential. Water Res. 46, 2225–2236. https://doi.org/10.1016/j.watres.2012.01.048.
Michener, R., Lajtha, K., 2007. Stable Isotopes in Ecology and Environmental Science. Tracing Anthropogenic Inputs of Nitrogen to Ecosystems. Blackwell Publishing, Hoboken, New Jersey.
Musgrove, M., Opsahl, S.P., Mahler, B.J., Herrington, C., Sample, T.L., Banta, J.R., 2016. Source, variability, and transformation of nitrate in a regional karst aquifer: Edwards aquifer, central Texas. Sci. Total Environ. 568, 457–469. https://doi.org/10.1016/j.scitotenv.2016.05.201.
Nestler, A., Berglund, M., Accoe, F., Duta, S., Xue, D.M., Boeckx, P., Taylor, P., 2011. Isotopes for improved management of nitrate pollution in aqueous resources: review of surface water field studies. Environ. Sci. Pollut. Res. 18, 519–533. https://doi.org/10.1007/s11356-010-0422-z.
Nguyet, V.T.M., Goldscheider, N., 2006. A simplified methodology for mapping groundwater vulnerability and contamination risk, and its first application in a tropical karst area, Vietnam. Hydrogeol. J. 14, 1666–1675. https://doi.org/10.1007/s10040-006-0069-5.
Panno, S.V., Hackley, K.C., Kelly, W.R., Hwang, H.H., 2006. Isotopic evidence of nitrate sources and denitrification in the Mississippi River, Illinois. J. Environ. Qual. 35, 495–504. https://doi.org/10.2134/jeq2005.0012.
Parkhurst, D.L., Appelo, C.A.J., 2013. Description of Input and Examples for PHREEQC Version 3—A Computer Program for Speciation, Batch-Reaction, One-Dimensional Transport, and Inverse Geochemical Calculations. Center for Integrated Data Analytics Wisconsin Science Center.
Parnell, A.C., Inger, R., Bearhop, S., Jackson, A.L., 2010. Source partitioning using stable isotopes: coping with too much variation. PLoS One 5, e9672. https://doi.org/10.1371/journal.pone.0009672.
Rivett, M.O., Buss, S.R., Morgan, P., Smith, J.W.N., Bemment, C.D., 2008. Nitrate attenuation in groundwater: a review of biogeochemical controlling processes. Water Res. 42, 4215–4232 (doi: https://doi.org/j.watres.2008.07.020).
Robinson, H.K., Hasenmueller, E.A., 2017. Transport of road salt contamination in karst aquifers and soils over multiple timescales. Sci. Total Environ. 603, 94–108. https://doi.org/10.1016/j.scitotenv.2017.05.244.
Saenz-de-Miera, O., Rosselló, J., 2014. Modeling tourism impacts on air pollution: the case study of PM_{10} in Mallorca. Tour. Manag. 40, 273–281. https://doi.org/10.1016/j.tourman.2013.06.012.
Schnegg, P.A., Costa, R., 2002. Tracer tests made easier with field fluorometers. Bull. Hydrogeol. 20, 89–91.
Sebela, S., Turk, J., 2014. Natural and anthropogenic influences on the year-round temperature dynamics of air and water in Postojna show cave, Slovenia. Tour. Manag. 40, 233–243. https://doi.org/10.1016/j.tourman.2013.06.011.
Simsek, S., Günay, G., Elhatip, H., Ekmekçi, M., 2000. Environmental protection of geothermal waters and travertines at Pamukkale, Turkey. Geothermics 29, 557–572. https://doi.org/10.1016/S0375-6505(00)00022-5.
Stanchev, H., Stancheva, M., Young, R., 2015. Implications of population and tourism development growth for Bulgarian coastal zone. J. Coast. Conserv. 19, 59–72. https://doi.org/10.1007/s11852-014-0360-x.
Stanford, B.D., Amoozegar, A., Weinberg, H.S., 2010. The impact of co-contaminants and septic system effluent quality on the transport of estrogens and nonylphenols through soil. Water Res. 44, 1598–1606. https://doi.org/10.1016/j.watres.2009.11.011.
Toor, G.S., Toor, M., Obrez, T., 2011. Onsite Sewage Treatment and Disposal Systems: An Overview. Institute of Food and Agricultural Sciences, University of Florida, Gainesville.
Tornevi, A., Bergstedt, O., Forsberg, B., 2014. Precipitation effects on microbial pollution in a river: lag structures and seasonal effect modification. PLoS One 29, e98546. https://doi.org/10.1371/journal.pone.0098546.
Umezawa, Y., Hosono, T., Onodera, S., Siringan, F., Buapeng, S., Delinom, R., Yoshimizu, C., Tayasu, I., Nagata, T., Taniguchi, M., 2008. Sources of nitrate and ammonium contamination in groundwater under developing Asian megacities. Sci. Total Environ. 404, 361–376 https://doi.org/j.scitote7nv.2008.04.021.
UNESCO, 2014. Decision: 38 COM 8B.9, South China Karst (China) (extension). http://whc.unesco.org/en/decisions/6094, Accessed date: 23 July 2018.
UNESCO, 2018a. World Heritage. http://whc.unesco.org/en/about, Accessed date: 23 July 2018.
UNESCO, 2018b. List of World Heritage in Danger. https://whc.unesco.org/en/danger, Accessed date: 23 July 2018.
United States Environmental Protection Agency (USEPA), 2002. Onsite Wastewater Treatment Systems Manual (EPA/625/R-00/008). Office of Water, Office of Research and Development, United States Environmental Protection Agency, Washington, D.C.
Van Beynen, P., Brinkmann, R., van Beynen, K., 2012. A sustainability index for karst environments. J. Cave Karst Stud. 74, 221–234.
Vesper, D.J., White, W.B., 2003. Metal transport to karst springs during storm flow: an example from Fort Campbell, Kentucky/Tennessee, USA. J. Hydrol. 276, 20–36. https://doi.org/10.1016/S0022-1694(03)00023-4.
Vesper, D.J., Loop, C.M., White, W.B., 2001. Contaminant transport in karst aquifers. Theor. Appl. Karstol. 13, 63–73.
Vías, J.M., Andreo, B., Perles, M.J., Carrasco, F., Vadillo, I., Jimenez, P., 2006. Proposed method for groundwater vulnerability mapping in carbonate (karstic) aquifers: the COP method. Hydrogeol. J. 14, 912–925. https://doi.org/10.1007/s10040-006-0023-6.
Wang, S., 2011. The New Method of Engineering Geology. Yinshengyingxiang Press, Beijing, China (in Chinese without English abstract).
Weng, T.N., Liu, C.W., Kao, Y.H., Hsiao, S.S.Y., 2017. Isotopic evidence of nitrogen sources and nitrogen transformation in arsenic-contaminated groundwater. Sci. Total Environ. 578, 167–185. https://doi.org/10.1016/j.scitotenv.2016.11.013.

Withers, P.J.A., Jordan, P., May, L., Jarvie, H.P., Deal, N.E., 2014. Do septic tank systems pose a hidden threat to water quality? Front. Ecol. Environ. 12, 123–130. https://doi.org/10.1890/130131.

Wu, Y., Jiang, Y., Yuan, D., Li, L., 2008. Modeling hydrological responses of karst spring to storm events: example of the Shuifang spring (Jinfo Mt., Chongqing, China). Environ. Geol. 55, 1545–1553. https://doi.org/10.1007/s00254-007-1105-z.

Yang, M., Hens, L., Ou, X., De Wulf, R., 2009. Tourism: an alternative to development? Mt. Res. Dev. 29, 75–81. https://doi.org/10.1659/Mrd.1051.

Yang, P.H., Yuan, D.X., Yuan, W.H., Kuang, Y.L., Jia, P., He, Q.F., 2010. Formations of groundwater hydrogeochemistry in a karst system during storm events as revealed by PCA. Chin. Sci. Bull. 55, 1412–1422. https://doi.org/10.1007/s11434-010-0083-9.

Yang, P., Ming, X., Groves, C., Sheng, T., 2018. Impact of hotel septic effluent on the Jinfoshan Karst aquifer, SW China. Hydrogeol. J. https://doi.org/10.1007/s10040-018-1890-3.

Yoder, J., Roberts, V., Craun, G.F., Hill, V., Hicks, L., Alexander, N.T., Radke, V., Calderon, R.L., Hlavsa, M.C., Beach, M.J., Roy, S.L., 2010. Surveillance for waterborne disease and outbreaks associated with drinking water and water not intended for drinking — United States, 2005–2006. Surveill. Summ. 57, 39–62. https://doi.org/10.1111/j.1745-6584.2010.00686.x.

Zhang, M.Q., Zhang, M.H., 2007. Assessing the impact of leather industries on the quality of water discharged into the East China Sea from Wenzhou Watersheds. J. Environ. Manag. 85, 393–403. https://doi.org/10.1016/j.jenvman.2006.10.016.

Zhu, Y., Ye, M., Roeder, E., Hicks, R.W., Shi, L.S., Yang, J.Z., 2016. Estimating ammonium and nitrate load from septic systems to surface water bodies within ArcGIS environments. J. Hydrol. 532, 177–192. https://doi.org/10.1016/j.jhydrol.2015.11.017.